

Removal of Atmospheric Pollutants

(6) Individual and Simultaneous Absorption of Dilute NO and SO₂ in Aqueous Slurries of MgSO₃ with Fe^{II}-EDTA

Ichibei KUDO, Takashi KONDO, Eizo SADA
and Hidehiro KUMAZAWA

大気汚染物質除去に関する研究

(6) EDTA・Fe(II)添加MgSO₃スラリーによる 希薄NO, SO₂の単一および同時吸収

工藤市兵衛・近藤高司・佐田栄三*・熊沢英博*

The absorption rates of (1) NO in aqueous solutions of Fe^{II}-EDTA, (2) NO in aqueous solutions or slurries of MgSO₃ with added Fe^{II}-EDTA, and (3) NO in the presence of SO₂ in aqueous slurries of MgSO₃ with added Fe^{II}-EDTA were measured using a stirred vessel with a plane gas-liquid interface at 25°C and 1 atm. The forward rate constant of the complexing reaction, NO+Fe^{II}-EDTA \rightleftharpoons Fe^{II}(EDTA)(NO), at various pH's was derived from the enhancement factor for absorption of NO in aqueous solutions of Fe^{II}-EDTA. The reduction of NO coordinated to Fe^{II}-EDTA with SO₃²⁻ is found to be very slow as compared with the above complexing reaction. Coexisting SO₂ can promote the absorption rate of NO by aqueous slurries of MgSO₃ with Fe^{II}-EDTA. It is believed that coexisting SO₂ plays a part of releasing SO₃²⁻ from the complex Fe^{II}(EDTA)(SO₃²⁻)(NO) and that the presence of SO₂ in the gas phase effectively improves the pH of the solution at the interface toward favorable values for the reaction of NO with Fe^{II}-EDTA.

Introduction

The removal of nitrogen oxides (NO_x) as well as sulfur oxides (SO_x) emitted from stationary combustion facilities has recently been required to protect the atmospheric environment. A number of wet and dry processes appropriate for the removal of NO_x have been developed and some wet scrubbing processes are capable of removing SO_x simultaneously. The wet scrubbing method, however, has a significant disadvantage of inevitable waste-liquor treatment. In considering such a drawback, it appears that aqueous solutions of Fe(II) chelate are promising liquid absorbents of NO because of easy regeneration.

In our previous paper (Sada et al., 1978a), the kinetics of absorption of NO in aqueous FeSO₄ solutions were checked for wide operating conditions, i.e., for exposure times of 0.2-5000 s and NO concentrations of 100 ppm-99% by volume using a wetted wall column, a quiescent liquid, and a stirred vessel with a plane gas-liquid interface. It was concluded that the chemical absorption process could be predicted satisfactorily by a theory of gas absorption with reversi-

ble reaction of the form of A+B \rightleftharpoons E. However, their absorption rates seem too low from the standpoint of practical application. Recently, it was shown that an aqueous solution of Fe^{II}-EDTA (ferrous ion coordinated to ethylenediaminetetraacetic acid) rapidly reacts with dissolved NO and has a very large absorption capacity for NO. Furthermore, it was reported that some reducing agents such as Na₂SO₃ can reduce NO coordinated to Fe^{II}-EDTA and a high absorption rate can be maintained.

It is one purpose of this paper to investigate the kinetics of the complexing reaction between NO and Fe^{II}-EDTA as well as the reduction of NO coordinated to Fe^{II}-EDTA with SO₃²⁻ by chemical absorption methods. To such an end, the absorptions of dilute NO in aqueous solutions of Fe^{II}-EDTA and in aqueous slurries of MgSO₃ with added Fe^{II}-EDTA were performed using a stirred vessel with a plane gas-liquid interface. From the experimental results on the former absorption system, the forward rate constant of the complexing reaction was determined, and it was deduced from those of the latter absorption

system that the reduction of NO coordinated to Fe^{II}-EDTA by SO₃²⁻ is very slow and occurs only in the bulk of the slurry. Therefore, conceivably sulfur dioxide coexisting with nitric oxide cannot reduce the absorption rate of nitric oxide. The merit of the usage of MgSO₃ slurry as a reducing agent is high absorption capacity for SO₂. Thus, it is considered that an aqueous slurry of MgSO₃ with Fe^{II}-EDTA is suitable for simultaneous treatment of NO and SO₂. An other purpose is to analyze the simultaneous absorption mechanism.

Experimental Section

Experiments were carried out on the following absorption system: (1) absorption of NO in aqueous solutions of Fe^{II}-EDTA, (2) absorption of NO, (3) absorption of SO₂, and (4) simultaneous absorption of NO and SO₂ in aqueous slurries of MgSO₃ with Fe^{II}-EDTA. The absorber was a stirred vessel with a plane gas-liquid interface (i.d. = 80mm, liquid volume = 500cm³), which was described in our previous paper (Sada et al., 1978a), and was operated continuously with respect to the gas phase and batchwise with respect to the liquid phase. Two stirres driven by two separate motors were used to agitate the gas and liquid phases. The liquid-phase and gas-phase stirrers were operated at constant speeds of 175 and 500 rpm, respectively.

The gas phase was dilute NO and/or SO₂. NO or SO₂ was supplied from a cylinder with 1.0% concentration, the balance being N₂. Both these gases were further diluted with N₂ to the desired concentration before being fed to the absorber. The feed concentrations of NO and SO₂ for the single absorption ranged from 40 to 1600 ppm and 580 to 3500 ppm, respectively, where as for the simultaneous absorption of NO and SO₂, the feed concentration of NO was varied from 40 to 630 ppm with that of SO₂ fixed at 500, 1050, 1500, and 3000 ppm.

The liquid phase was an aqueous solution of Fe^{II}-EDTA and an aqueous slurry of MgSO₃ with Fe^{II}-EDTA. The Fe^{II}-EDTA solutions were prepared by adding equimolar amounts of FeSO₄ and EDTA2Na (ethylenediaminetetraacetic acid disodium salt) to distilled water, and the pH of the solution was adjusted by aqueous ammonia. The concentration of Fe^{II}-EDTA ranged from 0.01 to 0.05 M. The concentration of MgSO₃ ranged from 0.5 to 5.0 wt %. The volume of the solution was always 500 cm³ and the gas flow rate was about 30 and 40 cm³/s.

The inlet and outlet gas-phase concentrations were determined by UV derivative spectrophotometer analyzer (Yanaco UO-1 derivative spectrophotometer). The absorption rate was determined from the inlet and outlet gas-phase concentrations and total gas flow rate.

During the experimental runs, the temperature was maintained at 25°C and the total pressure was 1 atm.

Results and Discussion

Experimental results are shown as a plot of absorption rate vs. interfacial concentration. Some of the observed absorption rates of NO were converted to enhancement factors by

$$N_A = k_{GA}(p_{AO} - p_{AI}) = k^*_{LA} \phi_A C_{AI} \quad (1)$$

Here, gas-side and liquid-side mass transfer coefficients, k_G and k_L , are obtained from empirical correlations described later. C_{AI} is liquid phase concentration of gaseous species A at equilibrium with p_{AI} . Then, eq 1 also enables one to derive the interfacial concentration of gaseous species.

The interfacial concentrations of NO and SO₂ in liquid absorbent were assumed to be equal to those in water because the concentrations of Fe^{II}-EDTA and SO₃²⁻ were relatively low under the experimental conditions considered here. The interfacial concentration of NO in liquid absorbent was estimated by assuming Henry's law ($H_{A3} = 1.92 \times 10^{-6} \text{mol/cm}^3 \cdot \text{atm}$ at 25°C (Kagaku Benran Kisohen, 1974a)), whereas the interfacial concentration of SO₂ was evaluated by using Fujita's equation (Fujita, 1963).

Liquid-Side and Gas-Side Mass Transfer Coefficients. The liquid-side mass transfer coefficient, k^*_{L} , was determined by measuring the rate of physical absorption of pure CO₂ into water at 25°C and correlated to the liquid phase stirring speed n_L by (Sada et al., 1978b)

$$k^*_{L,CO_2} = 9.41 \times 10^{-5} n_L^{0.65} \quad (2)$$

Under the experimental conditions for the dilute SO₂ absorption into aqueous solutions of NaOH, the overall mass transfer coefficient, K_G , was found to be independent of NaOH concentration. That is, $K_G = k_G$. The gas-side mass transfer coefficient, k_G , was correlated to the gas phase stirring speed n_G by

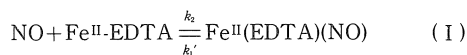
$$k_{G,SO_2} = 1.22 \times 10^{-6} n_G^{0.61} \quad (3)$$

The values of liquid-side and gas-side mass transfer coefficients for gaseous species I were calculated by the following correlations with experimental values of k^*_{L,CO_2} and k_{G,SO_2} , respectively.

$$k^*_{L1} = k^*_{L,CO_2} (D_1/D_{CO_2, H_2O})^{2/3} \quad (4)$$

$$k_{G1} = k_{G,SO_2} (D_1/D_{SO_2, N_2})^{2/3} \quad (5)$$

Absorption of NO into Aqueous Solutions of Fe^{II}-EDTA. Nitric oxide reacts with Fe^{II}-EDTA in aqueous solutions according to the complexing reaction



to form a complex compound. It is considered that the forward reaction is second order, i.e., first order in both NO and Fe^{II}-EDTA and the reverse reaction is first order in Fe^{II}(EDTA)(NO) as deduced from the

complexing reaction between NO and FeSO_4 in aqueous solutions (Kustin et al., 1966)

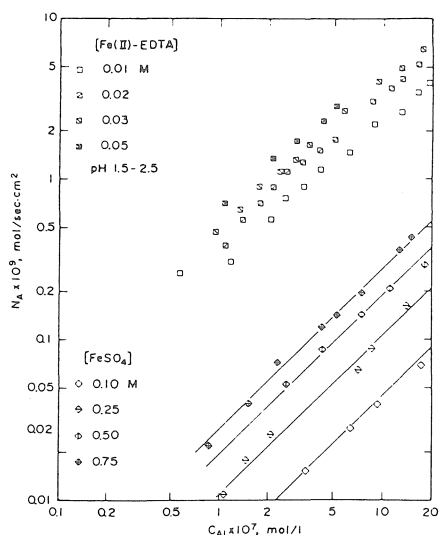


Figure 1. Absorption rates of NO in aqueous solutions of Fe^{II} -EDTA without adjusting pH.

The value of the chemical equilibrium constant of reaction I is in the order of 10^6 L/mol at 25°C (Teramoto et al., 1978) and is about four orders of magnitude over that of reaction II reported by Kustin et al. (1966).

Figure 1 shows a plot of the absorption rate of NO, N_A , against the interfacial concentration of NO in the liquid phase, C_{A1} . A group of straight lines with the slope of unity, which are plotted to the lower part of this figure, indicate the same relationship for the absorption of NO into aqueous solutions of FeSO_4 (Sada et al., 1978a). The values of the rate constant of the forward reaction k_2 and the chemical equilibrium constant K for the NO- FeSO_4 system are much lower than those for the NO- Fe^{II} -EDTA system. (Kustin et al. (1966) reported $K = 450$ L/mol and $k_2 = 6.2 \times 10^5$ L/mols at 25°C for the former system.) Thus, the process of the absorption of NO into aqueous solutions of FeSO_4 using a stirred vessel with a plane gas-liquid interface lies in the instantaneous (equilibrium) reaction regime and the logarithmic plot of N_A vs. C_{A1} has a slope of unity (Sada et al., 1978a), whereas the slope of the same plot for the NO- Fe^{II} -EDTA is lower than unity, indicating that the chemical absorption process lies in a transition region between fast and instantaneous reactions. Experimental rates of absorption by aqueous Fe^{II} -EDTA solutions (pH 7 and 9.5-10, respectively) were shown in Figures 2 and 3. The slope of the plot of $\log N_A$ vs. $\log C_{A1}$ in these figures is also smaller than unity. Figures 1 through 3 indicate that N_A has a maximum at some pH close to 7.

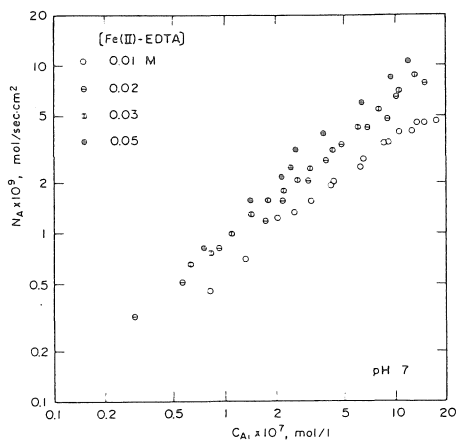


Figure 2. Absorption rates of NO in aqueous solutions of Fe^{II} -EDTA at pH 7.

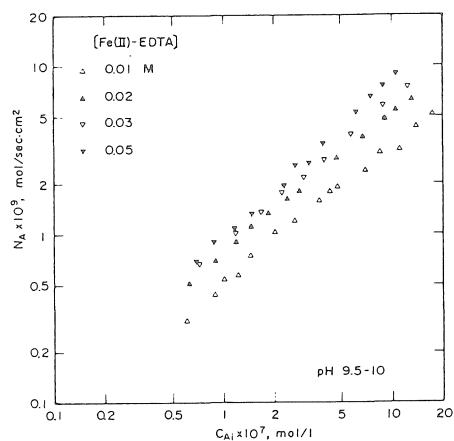


Figure 3. Absorption rates of NO in aqueous solutions of Fe^{II} -EDTA at pH 9.5-10.

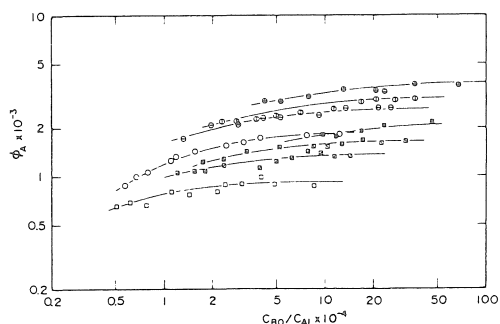


Figure 4. Enhancement factors for absorption of NO in aqueous Fe^{II} -EDTA solutions as a function of C_{B0}/C_{A1} .

Figure 4 shows the relation of the enhancement factor ϕ_A derived from the absorption rate of NO in Figures 1 and 2 to C_{B0}/C_{A1} . As C_{B0}/C_{A1} increases, ϕ_A approaches a constant value, depending upon C_{B0} . This asymptotic value can be considered the enhancement factors lying in a fast-reaction regime, where ϕ_A equals $M^{1/2}$.

Table I. Forward Rate Constant of Complexing Reaction (I) from Chemical Absorption Data at 25 °C

pH	C_{B_0} , mol/L	$(\phi_A)_{C_{B_0}/C_{A_1} \rightarrow \infty}$	k_1 L/mol s	$(k_1)_{av}$, L/mol s
1.5-2.5	0.01	930	3.15×10^7	$(3.29 \pm 0.18) \times 10^7$
	0.02	1380	3.47×10^7	
	0.03	1660	3.34×10^7	
	0.05	2100	3.21×10^7	
7	0.01	1900	1.31×10^8	$(1.23 \pm 0.06) \times 10^8$
	0.02	2600	1.23×10^8	
	0.03	3100	1.17×10^8	
	0.05	4000	1.17×10^8	
	0.01	1650	9.91×10^7	
9.5-10	0.02	2500	1.14×10^8	$(1.04 \pm 0.10) \times 10^8$
	0.03	2960	1.06×10^8	
	0.05	3620	9.54×10^7	

$$\phi_A = M^{1/2} = (k_2 C_{B_0} D_A)^{1/2} / k_{LA} \quad (6)$$

Therefore, the forward rate constant of the complexing reaction I, k_2 , can be derived from eq 6. The values of k_2 thus calculated at various pH's are shown in Table I. The complexing reaction rate is the greatest when the pH is close to 8.

Absorption of NO into Aqueous Slurries of $MgSO_3$ with Fe^{II} -EDTA. If the reaction product of a reversible reaction is consumed by another reaction, the reversible reaction can proceed irreversibly. Hence, it is expected that the absorption rate of NO with added SO_3^{2-} may be faster than that without added SO_3^{2-} because the nitric oxide coordinated to Fe^{II} -EDTA can be reduced by SO_3^{2-} . The experimental results on the absorption of NO into aqueous solutions or aqueous slurries of $MgSO_3$ with Fe^{II} -EDTA are shown in Figure 5. It is proved that the

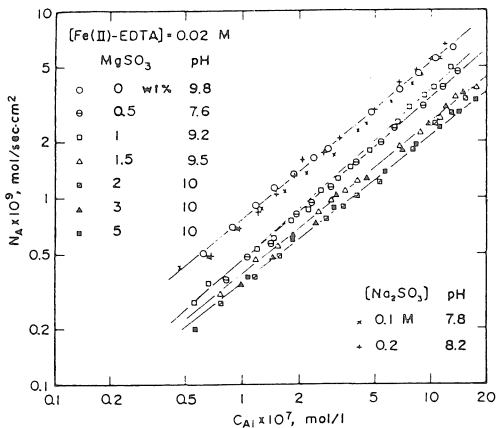


Figure 5. Absorption rates of NO in aqueous solutions or slurries of $MgSO_3$ with added Fe^{II} -EDTA.

absorption rates with added $MgSO_3$ are low compared with those into aqueous solutions of Fe^{II} -EDTA adjusted at pH 9.8. The absorption rates of NO into aqueous mixed solutions of Fe^{II} -EDTA and Na_2SO_3 are also plotted in this figure. In this case, also, the absorption rates do not exceed those into aqueous solutions of Fe^{II} -EDTA at pH 9.8. The slope of plotted relationship between $\log N_A$ and $\log C_{A_1}$ is clearly smaller than unity, suggesting that the chemi-

cal absorption process does not lie in a fast-reaction regime. Thus, the rate of reduction of NO coordinated to Fe^{II} -EDTA with SO_3^{2-} is very slow compared with the complexing reaction (I) and can be apparently neglected.

Simultaneous Absorption of NO and SO_2 into Aqueous Slurries of $MgSO_3$ with Fe^{II} -EDTA. Figure 6 represents results on the absorption of SO_2 into aqueous slurries of $MgSO_3$ with added Fe^{II} -EDTA. These results have been plotted as absorption rate N_A , vs. gas phase partial pressure of SO_2 , $P_{A,0}$. The

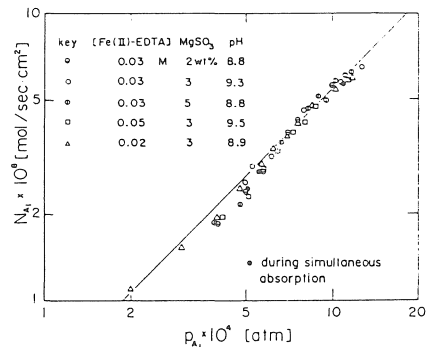


Figure 6. Absorption rates of SO_2 in aqueous slurries of $MgSO_3$ with added Fe^{II} -EDTA.

solid line represents the absorption rate under completely gas-film controlled conditions. It can be seen that the absorption process of SO_2 into the aqueous slurry is almost gas-film controlled under the partial pressures in the present experiment. Thereby, the rate of absorption is independent of solid concentration in the slurry solution. Full circular points in this figure denote absorption rates of SO_2 during the simultaneous absorption of NO and SO_2 in the same slurries, and coincide with those under the completely gas-film controlled conditions.

Experimental results on the simultaneous absorption of NO and SO_2 into the aqueous slurries were shown in Figures 7 and 8. These results have been plotted in terms of absorption rate of NO, $N_{A,1}$, against interfacial concentration of NO, $C_{A,i}$, with inlet SO_2 concentration as a parameter. The solid lines and open circles represent absorption rates of

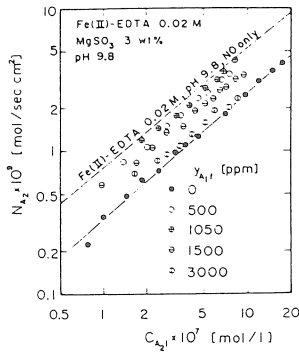


Figure 7. Absorption rates of NO in aqueous slurries of MgSO₃ with added Fe^{II}-EDTA at 0.02 M.

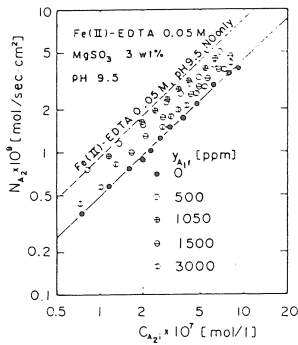
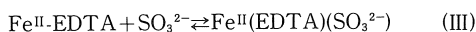


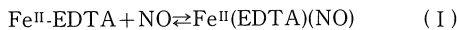
Figure 8. Absorption rates of NO in aqueous slurries of MgSO₃ with added Fe^{II}-EDTA at 0.05 M.

NO in the absence of SO₂, which are taken from Figure 5. The experimental absorption rates of NO in the presence of SO₂ fall much above the solid lines. The degree of promotion in absorption rates of NO in the presence of SO₂ tends to decrease with increasing SO₂ concentration. However, they do not decline to the broken lines which show rates of single NO absorption into aqueous Fe^{II}-EDTA solutions containing no MgSO₃ at pH 9.8 and 9.5. In any event, it is noted that coexisting SO₂ could promote the absorption rate of NO by an aqueous slurry of MgSO₃ with Fe^{II}-EDTA.

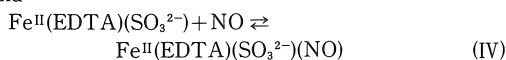
Recently, Teramoto et al. (1978) proposed a mechanism of the reaction between NO and an aqueous mixed solution of Fe^{II}-EDTA and Na₂SO₃ as follows. When Na₂SO₃ is added to an aqueous Fe^{II}-EDTA solution, there exists an interaction such as



Thus, when NO is absorbed into an aqueous mixed solution of Fe^{II}-EDTA and Na₂SO₃, NO may coordinate to Fe(II) according to

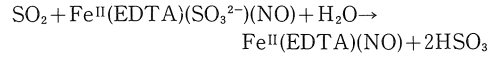


and



to form Fe^{II}(EDTA)(NO) and Fe^{II}(EDTA)(SO₃²⁻)(NO). The complex Fe^{II}(EDTA)(NO) is easily reduced by Na₂SO₃, whereas the complex Fe^{II}(EDTA)(SO₃²⁻)(NO) must release SO₃²⁻ in order to be easily reduced by Na₂SO₃.

In the present simultaneous absorption runs, coexisting SO₂ plays a part of releasing SO₃²⁻ from the complex Fe^{II}(EDTA)(SO₃²⁻)(NO).



Therefore, the rate of absorption of NO during the simultaneous absorption of NO and SO₂ is higher than the rate of the single NO absorption. The reaction product HSO₃⁻ is accumulated near the gas liquid interface and decreases the pH near the interface to about 7. The reaction between NO and Fe^{II}-EDTA is maximum near pH 8 as shown in Table I.

Figures 7 and 8 have indicated that the rate of NO absorption during the simultaneous absorption decreases with an increase in the concentration of SO₂ in the gas phase. This is due to decreasing the pH near the interface, which is deduced as follows.

When SO₂ is absorbed under the completely gas-film controlled conditions, the interfacial concentrations of SO₃²⁻ and HSO₃⁻ can be estimated from the material balances at the interface

$$N_{A_i} = N_E = N_F/2 \quad (7)$$

Here

$$N_{A_i} = k_{GA_i} p_{A_i} \quad (8)$$

$$N_E = k_{LE}^*(C_{E_s} - C_{E_i})N^{1/2} \coth N^{1/2} \quad (9)$$

$$N_F = k_{LF}^* C_{F_i} \quad (10)$$

Derivation of eq 9 is given in the Appendix.

The values of k_G and k_L^* can be estimated by eq 2-4. C_{E_s} is 6.18×10^{-2} mol/L, which is calculated from solubility of MgSO₃ in water at 25°C. The value of N for 3 wt % slurry is assumed to be 0.78, considering a series of our experimental work on chemical absorption by slurry (Sada et al., 1979). The interfacial concentrations of SO₃²⁻ and HSO₃⁻ calculated from such estimates are tabulated in the second and third columns in Table II. As the equilibrium constant of ionic reaction $\text{HSO}_3^- \rightleftharpoons \text{H}^+ + \text{SO}_3^{2-}$, is 6.2×10^{-8} L/g-ion at 25°C (Kagaku Benran Kisoheh, 1974b), the interfacial concentration of H⁺, and therefore pH can be calculated on the fourth and fifth columns, respectively. The values of pH decrease with an increase in SO₂ partial pressure. The presence of SO₂ in the gas phase effectively changes the pH at the interface toward favorable values to the reaction of NO with Fe^{II}-EDTA.

Table II. Interfacial Concentrations of SO₃²⁻, HSO₃⁻, and H⁺

Y_{A_i} , ppm	C_{E_i} , g-ion/L	C_{F_i} , g-ion/L	$[\text{H}^+]$, g-ion/L	pH
500	5.75×10^{-2}	1.10×10^{-2}	1.18×10^{-8}	7.93
1050	5.08×10^{-2}	2.83×10^{-2}	3.45×10^{-8}	7.46
1500	4.86×10^{-2}	3.40×10^{-2}	4.34×10^{-8}	7.36
3000	3.83×10^{-2}	7.21×10^{-2}	1.17×10^{-7}	6.93

Conclusion

The absorption of (1) NO in aqueous solutions of Fe^{II}-EDTA, (2) NO in aqueous solutions or slurries of MgSO₃ with added Fe^{II}-EDTA, and (3) NO in the presence of SO₂ in aqueous slurries of MgSO₃ with added Fe^{II}-EDTA were carried out using a stirred vessel with a plane gas-liquid interface at 25°C and 1 atm. The forward rate constant of complexing reaction, $\text{NO} + \text{Fe}^{\text{II}}\text{-EDTA} \rightleftharpoons \text{Fe}^{\text{II}}(\text{EDTA})(\text{NO})$, at various pH was derived from enhancement factors lying in a fast-reaction regime for system 1. It is found from system 2 that the reduction of NO coordinating to Fe^{II}-EDTA with SO₃²⁻ is very slow compared with the above complexing reaction and apparently can be neglected. The absorption rate of NO in the presence of SO₂ considerably exceeded that in the absence of SO₂. It is believed that coexisting SO₂ plays a part of releasing SO₃²⁻ from the complex Fe^{II}(EDTA)(SO₃²⁻)(NO) and that the presence of SO₂ effectively reduces the pH of the solution at the interface toward favorable values to the complexing reaction of NO with Fe^{II}-EDTA.

Appendix

The mass balance equation incorporating the effect of simultaneous solid dissolution is written by

$$D_E \frac{d^2 C_E}{dz^2} + k_s A_p (C_{Es} - C_E) = 0 \quad (\text{A1})$$

The boundary conditions are

$$\text{at } z = 0 \quad C_E = C_{E1} \quad (\text{A2})$$

$$\text{at } z = z_L \quad C_E = C_{Es} \quad (\text{A3})$$

The mass balance equation in the dimensionless form reduces to

$$\frac{d^2 Y_E}{dx^2} + N(1 - Y_E) = 0 \quad (\text{A4})$$

with the boundary conditions

$$\text{at } x = 0 \quad Y_E = Y_{E1} \quad (\text{A5})$$

$$\text{at } x = 1 \quad Y_E = 1 \quad (\text{A6})$$

Solution of eq A4 gives the dimensionless concentration profile

$$Y_E = (1 - Y_{E1}) \frac{\coth N^{1/2} \sinh(N^{1/2}x) - (1 - Y_{E1}) \cosh(N^{1/2}x) + 1}{(1 - Y_{E1}) \cosh(N^{1/2}x) + 1} \quad (\text{A7})$$

The rate of diffusion of the solid component toward the interface is obtained by

$$\begin{aligned} N_E &= D_E (dC_E/dz)_{z=0} \\ &= (D_E C_{Es}/z_L) (dY_E/dx)_{x=0} \\ &= k_{LE}^* (C_{Es} - C_{E1}) N^{1/2} \cosh N^{1/2} \quad (\text{A8}) \end{aligned}$$

Nomenclature

- A_p = surface area of solid particles, $6w/pd_p$, cm²/cm³ of disperson
 C = concentration in liquid phase, mol/cm³ or mol/L
 D = diffusivity in liquid phase, cm²/s
 \mathcal{D} = diffusivity in gas phase, cm²/s
 d_p = average diameter of solid particles, cm
 k = second-order forward rate constant of complexing reaction, L/mol s
 k' = first-order reverse rate constant of complexing reaction, 1/s
 K_G = overall gas-side mass transfer coefficient, mol/s cm² atm
 k_G = gas-side mass transfer coefficient, mol/s cm² atm
 k_L = liquid-side mass transfer coefficient, cm/s
 k_s = mass transfer coefficient for solid dissolution, cm/s
 M = reaction-diffusion modulus, $k_2 C_{B0} D_A / (k_{LA}^*)^2$
 N = $k_s A_p z_L^2 / D_E$
 N_i = mass transfer rate of component I, mol/s cm²
 n_G = agitation speed in gas phase, rpm
 n_L = agitation speed in liquid phase, rpm
 p = partial pressure, atm
 w = concentration of solid, g/cm³ of disperson or wt %
 x = dimensionless distance into liquid phase from gas-liquid interface, z/z_L
 $Y_E = C_E/C_{Es}$
 y = gas-phase concentration, ppm
 z = distance into liquid phase from gas-liquid interface, cm
 z_L = thickness of liquid film for gas absorption, cm

Greek Letters

- ρ = density of solid, g/cm³
 ϕ = enhancement factor

Subscripts

- A = NO
 A_1 = SO₂
 A_2 = NO
 B = Fe^{II}-EDTA
 E = MgSO₃ or SO₃²⁻
 F = HSO₃⁻
 f = feed stream
 i = gas-liquid interface
 0 = effluent stream
 s = surface of solid particle

Superscript

- ° = without chemical reaction

Literature Cited

- Fujita, S., *Kagaku Kogaku*, **27**, 109 (1963).
"Kagaku Benran Kisohen", p 770, Japan Chemical Society, Maruzen, Tokyo, 1974a.
"Kagaku Benran Kisohen", p 994, Japan Chemical Society, Maruzen, Tokyo, 1974b.
Kustin, K., Taub, I. A., Weinstock, E., *Inorg. Chem.*, **5**, 1079 (1966).
Sada, E., Kumazawa, H., Tsuboi, N., Kudo, I., Kondo, T., *Ind. Eng. Chem. Process Des. Dev.*, **17**, 321 (1978a).
Sada, E., Kumazawa, H., Kudo, I., Kondo, T., *Chem. Eng. Sci.*, **33**, 315 (1978b).
Sada, E., Kumazawa, H., Butt, M. A., *J. Chem. Eng. Jpn.*, **12**, 111 (1979).
Teramoto, M., Hiramane, S., Shimada, Y., Sugimoto, Y., Teranishi, H., *J. Chem. Eng. Jpn.*, **11**, 450 (1978).

(受理 昭和56年1月16日)